Zinc-dependent and independent actions of hydroxyhydroquinone on rat thymic lymphocytes

Honoka Wada[1], Keisuke Oyama[2], Risa Kamae[1], Toshiya Masuda[3], Kaori Kanemaru[1,4], Kumio Yokoigawa[1,4], Yasuo Oyama[1,4,*]

[1] Faculty of Integrated Arts and Sciences, Tokushima University, Tokushima 770-8502, Japan

[2] Intensive Care Unit, Osaka University Hospital, Suita 565-0871, Japan

[3] Graduate School of Human Life Science, Osaka City University, Osaka 558-8585, Japan

[4] Faculty of Bioscience and Bioindustry, Tokushima University, Tokushima 770-8513, Japan

Running Head: Zinc-dependent and independent actions of hydroxyhydroquinone

[*] Corresponding author: Yasuo Oyama, Ph.D. E-mail: oyamay@tokushima-u.ac.jp

Highlights

• Hydroxyhydroquinone (HHQ) is known as a by-product of coffee bean roasting.

• HHQ at sublethal levels increased intracellular Zn^{2+} concentration in rat thymocytes.

• HHQ at higher levels decreased cellular glutathione content.

• HHQ protected the cells against H_2O_2-induced oxidative stress.

• HHQ exerts contrasting cellular actions related to redox status.

Abstract

Coffee contains hydroxyhydroquinone (HHQ). HHQ is one of by-products released during bean roasting. Therefore, it is important to elucidate the bioactivity of HHQ to predict its beneficial or adverse effects on humans. We studied zinc-dependent and independent actions of commercially-procured synthetic HHQ in rat thymocytes using flow cytometric techniques with propidium iodide, FluoZin-3-AM, 5-chloromethylfluorescein diacetate, and annexin V-FITC. HHQ at 1050 μM elevated intracellular Zn^{2+} levels by releasing intracellular Zn^{2+}. HHQ at 10 μM increased cellular thiol content in a Zinc-dependent manner. However, HHQ at 30–50 μM reduced cellular thiol content. Although the latter actions of HHQ (30–50 μM) were suggested to increase cell vulnerability to oxidative stress, HHQ at 0.3–100 μM significantly protected cells against oxidative stress induced by H_2O_2. The process of cell death induced by H_2O_2 was delayed by HHQ, although both H_2O_2 and HHQ increased the population of annexin V-positive living cells. However, HHQ at 10–30 μM promoted cell death induced by A23187, a calcium ionophore. HHQ at 10–30 μM exerted contrasting effects on cell death caused by oxidative stress and Ca^{2+} overload. Because HHQ is considered to possess diverse cellular actions, coffee with reduced amount of HHQ may be preferable to avoid potential adverse effects.

Keywords: hydroxyhydroquinone; zinc; oxidative stress; glutathione; lymphocytes

Introduction

Hydroxyhydroquinone (HHQ) is a by-product of coffee bean roasting (Müller et al, 2006). A cup of coffee contains 0.1–1.7 mg of HHQ (Ochiai et al., 2008). Coffee is a popular beverage, and thus, a large amount of HHQ may be ingested per day. It is important to elucidate the biological actions of HHQ to predict its beneficial or adverse effects on humans. In our previous study (Kamae et al., 2017) using Fluo-3, a fluorescent indicator of intracellular Ca^{2+}, HHQ increased intracellular Ca^{2+} concentration ($[Ca^{2+}]_i$) in rat thymocytes, potentially leading to cell death. We also found that the application of a chelator of intracellular Zn^{2+} further increased the intensity of Fluo-3 fluorescence in the presence of 50 μM HHQ, suggesting that Zn^{2+} interfered with Ca^{2+} binding to Fluo-3. In addition, 50 μM HHQ augmented FluoZin-3 fluorescence, an indicator of intracellular Zn^{2+} concentration ($[Zn^{2+}]_i$), indicating that $[Zn^{2+}]_i$ was increased by HHQ. Since our previous study was conducted to examine the contribution of intracellular Ca^{2+} to the cytotoxicity of HHQ, basic information on the HHQ-induced elevation of $[Zn^{2+}]_i$, such as threshold concentration (concentration-response relation), mechanism of action, and toxicological (or pharmacological) implications, were totally lacking. Therefore, in this study, we revealed the Zinc-dependent and independent actions of HHQ because of following reasons. Zn^{2+} has many physiological roles as an intracellular signal (Haase and Rink, 2014; Hojyo and Fukada, 2016). Dyshomeostasis of $[Zn^{2+}]_i$ is proposed to trigger pathological events (Park et al, 2014; Yoo et al., 2016). Furthermore, zinc potentiated the cytotoxicity of some biocidal chemicals such as imidazole antifungals, isothiazolinone preservatives, and hydrogen peroxide under in vitro conditions (Matsui et al., 2008, 2010; Fukunaga et al., 2015; Saitoh et al., 2015). Therefore, we also examined the effects of HHQ on the increase in cell lethality respectively induced by oxidative stress and intracellular Ca^{2+} overload.

In this study, cellular actions of sublethal concentrations of HHQ were examined using flow cytometric techniques with appropriate fluorescent dyes in rat thymocytes. Thymus is most

active during neonatal and pre-adolescent periods and this organ begins to atrophy by early teens. Since many people are concerned about the adverse effects of chemical compounds on the health of their children, the results obtained from thymocytes scientifically draw interest of people. Furthermore, in technical aspects, the cells with intact membranes could be obtained because no enzymatic treatment was required to isolate individual cells. Several types of chemical and biological substances cause cell death in thymocytes (Corsini et al., 2013; Kuchler et al., 2014; Solti et al., 2015) and the process of cell death (apoptosis, necrosis, and autophagy) has been well studied (Klein et al., 2014; Poon et al., 2014; Shimizu et al, 2014).

Materials and methods

Chemical

HHQ (99.9 % purity) used in this study was purchased from Tokyo Chemical Industry Co., Ltd. (Tokyo, Japan). Zn^{2+} chelators for extracellular and intracellular Zn^{2+} (Tab. 1) were supplied by Dojin Chemical Laboratory (Kumamoto, Japan). Fluorescent probes for examining membrane and cellular parameters (Tab. 1) were obtained from Invitrogen (Eugene, OR, USA). Other chemicals were obtained from Wako Pure Chemicals (Osaka, Japan) unless mentioned.

(Table 1 near here)

Animals and cell preparation

This study (Registered No. 05279 and T29-52) was approved by the Tokushima University Committee for Animal Experiments (Tokushima, Japan). The cell suspension was prepared as previously reported (Matsui et al., 2010). In brief, thymus glands were obtained from rats that were anesthetized with ether. Slices of glandular tissue were gently triturated in cold Tyrode's

solution (2–4 °C, 150 mM NaCl, 5 mM KCl, 2 mM $CaCl_2$, 1 mM $MgCl_2$, 5 mM glucose, pH 7.4 adjusted by 5 mM 4-(2-hydroxyethyl)-1-piperazineethanesulfonic acid and an appropriate amount of NaOH) to dissociate single thymocytes. The solution containing dissociated cells was then passed through a mesh (56 μm in diameter) to prepare a cell suspension. It was noted that the cell suspension contained 216.9 ± 14.4 nM zinc that was derived from the cell preparation process (Sakanashi et al., 2009). The cell suspension was incubated at 36–37 °C for 1 h before any experimentation.

Drug application

Various concentrations of HHQ (0.3–100 mM in dimethyl sulfoxide) were added to the cell suspension (2 mL per test tube) for achieving final concentrations of 0.3-100 μM and thereafter the cells were incubated with HHQ at 36–37 °C for 1–3 h. The incubation time varied according to the experimental purpose. A sample from each cell suspension (100 μL) was analyzed by flow cytometry to estimate the HHQ-induced changes in cellular and membrane parameters. It took 10–15 s to acquire data from 2500 cells. Cell viability estimated from 2500 cells was quite similar to that estimated from 10000 cells. Therefore, 2500 cells were enough to examine cellular actions of HHQ.

Fluorescence measurements

Cellular and membrane parameters were measured using a flow cytometer equipped with an argon laser (CytoACE-150; JASCO, Tokyo, Japan) and fluorescent probes, as previously described (Matsui et al., 2008). The fluorescence was analyzed by JASCO operating system software (Version 3.06; JASCO, Tokyo, Japan). Under experimental conditions, no fluorescence from the reagents used was observed, except for the fluorescent probes. The

excitation wavelength for all fluorescent probes used in this study was 488 nm, while emissions wavelengths were 530 ± 20 nm for FluoZin-3 and 5-CMF, and 600 ± 20 nm for PI. To assess cell lethality, PI was added to the cell suspensions to a final concentration of 5 μM. Because PI stains dead cells, the measurement of PI fluorescence provides information on cell lethality. Fluorescence was measured using a flow cytometer 2 min after adding PI. FluoZin-3-AM was used to monitor changes in the intracellular Zn^{2+} levels ($[Zn^{2+}]_i$) (Gee et al., 2002). The cells were treated with 1 μM FluoZin-3-AM for 60 min prior to any fluorescence measurements. FluoZin-3 fluorescence was monitored from the cells without PI fluorescence. 5-CMF-DA was used to estimate the cellular content of glutathione ($[GSH]_i$) in rat thymocytes (Chikahisa et al., 1996). The 5-CMF fluorescence was measured 30 min after adding 1 μM 5-CMF-DA because it attains peak intensity within 30 min after application. Living cells that were not stained with PI were examined for 5-CMF fluorescence. Zn^{2+}-free condition was prepared by adding Zn^{2+} chelator (DTPA or TPEN) to the cell suspension 10 min at least before the experiments. Because DTPA is not membrane-permeable, DTPA chelates extracellular Zn^{2+}. Membrane-permeable TPEN can chelate intracellular Zn^{2+}.

Statistical analysis and presentation

Statistical analyses were done using ANOVA, with post-hoc Tukey's multivariate analysis. P-values of 0.05 or less were considered statistically significant. In describing the results, values (columns and bars in figures) were expressed as the mean and the standard deviation (SD) of 4–8 samples. Each experiment was repeated three times unless noted otherwise.

Results

HHQ-induced increase in $[Zn^{2+}]_i$

The treatment of cells with 10 μM and 30 μM HHQ for 1 h shifted FluoZin-3 fluorescence histogram in the direction of higher intensity (Fig. 1A). Thus, all cells responded to HHQ, resulting in augmented FluoZin-3 fluorescence. Dose-dependent increases in mean intensity of FluoZin-3 fluorescence were observed in the cells treated with 3–50 μM HHQ for 1 h (Fig. 1B). Augmentation of FluoZin-3 fluorescence by HHQ at 10 μM or more (up to 50 μM) was statistically significant. Thus, HHQ at 10 μM or more was found to significantly increase $[Zn^{2+}]_i$.

(Figure 1 near here)

HHQ-induced release of intracellular Zn^{2+}

Zn^{2+} chelators were used to investigate potential sources of Zn^{2+} for the HHQ-induced increase in $[Zn^{2+}]_i$. HHQ at 30 μM significantly augmented FluoZin-3 fluorescence even in the presence of 10 μM DTPA, that chelates extracellular Zn^{2+} (Fig. 2). Thus, it is likely that HHQ increased $[Zn^{2+}]_i$ upon removal of external Zn^{2+}. The increase in FluoZin-3 fluorescence in the presence of DTPA was approximately similar to that in its absence (Fig. 2), indicating little contribution by external Zn^{2+}. The HHQ-induced increase in FluoZin-3 fluorescence was eliminated when intracellular Zn^{2+} was chelated with 10 μM TPEN (Fig. 2). Therefore, we hypothesize that HHQ increased $[Zn^{2+}]_i$ independent of external Zn^{2+}. Release of Zn^{2+} from cellular stores may be responsible for the HHQ-induced increase in $[Zn^{2+}]_i$.

(Figure 2 near here)

HHQ-induced change in $[GSH]_i$

Decreased cellular nonprotein thiol content, primarily GSH, is one of indicators of oxidative stress. Furthermore, intracellular Zn^{2+} forms a complex with cellular thiols, and thiols convert

disulfide under oxidative stress, resulting in intracellular Zn^{2+} release. To study the effects of HHQ on $[GSH]_i$, 5-CMF fluorescence was recorded from the cells treated with 10–50 μM HHQ. The treatment with 10 μM HHQ for 1 h augmented mean 5-CMF fluorescence intensity, while significant fluorescence attenuation was observed in the cases of 30–50 μM HHQ (Fig. 3).

The effect of HHQ was also tested in the presence of TPEN, a chelator of intracellular Zn^{2+}, to determine whether Zn^{2+} was involved in 5-CMF fluorescence augmentation. In the presence of TPEN, the treatment with 10 μM HHQ did not increase 5-CMF fluorescence, while the same reduction in fluorescence intensity was detected in the cases of 30–50 μM HHQ (Fig. 3). We propose that intracellular Zn^{2+} is responsible for the elevation of [GSH]i by 10 μM HHQ.

(Figure 3 near here)

Effects of HHQ on cells simultaneously treated with H_2O_2

The increase in $[Zn^{2+}]_i$ by HHQ has contrasting effects, dependent on cellular redox status. Thus, it is difficult to predict HHQ effects on cells under oxidative stress. Therefore, the effects of 0.3–30 μM HHQ on cells treated with 100 μM H_2O_2 were examined. The cells were co-treated with H_2O_2 and HHQ for 3 h. Thereafter, cell lethality was examined with PI staining. Treatment of cells with 100 μM H_2O_2 for 3 h significantly increased cell lethality from 5.4 ± 0.8 % to 19.3 ± 1.5 % (Fig. 4). Simultaneous application of HHQ at concentrations ranging from 0.3 μM to 30 μM significantly attenuated H_2O_2-induced increases in cell lethality in dose-dependent manner (Fig. 4). The inhibitory action of HHQ was maximized at concentrations of 10–30 μM. Further increases in HHQ concentration to 100 μM did not produce further inhibition. Thus, HHQ appears to protect cells against oxidative stress elicited by H_2O_2.

(Figure 4 near here)

HHQ-induced inhibition of death of living cells with exposed PS

Both HHQ and H_2O_2 are assumed to initiate the process of cell death. However, as described above, co-treatment with HHQ and H_2O_2 did not result in additive or synergistic actions. As shown in Fig. 5A, HHQ (100 μM) and H_2O_2 (100 μM) greatly increased the proportions of cells with FITC fluorescence and without PI fluorescence, respectively. In the case of H_2O_2, cells with PI fluorescence were also significantly more abundant. However, in cells co-treated with HHQ and H_2O_2, the proportions of cells exhibiting PI fluorescence, and those with FITC but without PI fluorescence were slightly, but significantly, less increased in comparison with cells treated with H_2O_2 alone (Fig. 5B). It is inferred that HHQ delays the process of cell death induced by H_2O_2.

(Figure 5 near here)

Effect of $ZnCl_2$ on cells treated with sublethal levels of HHQ

HHQ at 30 μM decreased $[GSH]_i$ (Fig. 3), suggesting a reduction in nonprotein thiols which maintain cellular Zn^{2+} homeostasis. Since HHQ at 10–30 μM itself increased $[Zn^{2+}]_i$ (Fig. 2), an excessive increase in $[Zn^{2+}]_i$ by HHQ was expected. Cells were co-treated with HHQ (10 or 30 μM) and $ZnCl_2$ (3 or 10 μM) for 3 h. The cell lethality of the control group was 7.1 ± 1.0 %, while it was less than 10 % for any combination of HHQ and $ZnCl_2$. Therefore, it is unlikely that $ZnCl_2$ greatly augments the action of HHQ.

Effect of HHQ on cells treated with A23187

Cells were treated with 100 nM A23187 for 3 h, resulting in a Ca^{2+}-dependent increase in cell lethality (Fig. 6). The co-treatment of cells with A23187 and 10–30 μM HHQ further increased cell lethality (Fig. 6). Thus, it appears that HHQ at 10–30 μM HHQ significantly augments Ca^{2+}-dependent cell death.

(Figure 6 near here)

Discussion

Zinc-dependent and independent cellular actions of HHQ

It is likely that HHQ at concentrations of 10 μM or more increases $[Zn^{2+}]_i$ in all cells because HHQ shifted the histogram of FluoZin-3 fluorescence in the direction of higher intensity (Fig. 1). The increase in $[Zn^{2+}]_i$ by HHQ is assumed to largely result from Zn^{2+} release from intracellular stores because DTPA, a chelator of external Zn^{2+}, only slightly attenuated the HHQ-induced augmentation of FluoZin-3 fluorescence (Fig. 2). Intracellular Zn^{2+} release could be caused by zinc-thiol/disulfide interchange, because Zn^{2+} binds to sulfhydryl groups and Zn^{2+} bound to thiols is released by oxidative stress (Maret, 2009). HHQ at 30–50 μM significantly reduced the intensity of 5-CMF fluorescence (Fig. 3), indicating a reduction of $[GSH]_i$. There was a discrepant observation in the case of 10 μM HHQ (Figs. 1 and 3). HHQ at 10 μM augmented both FluoZin-3 fluorescence and 5-CMF fluorescence, indicating that HHQ induced increases in both $[Zn^{2+}]_i$ and $[GSH]_i$. The augmentation of 5-CMF fluorescence by HHQ was not observed in the presence of TPEN, a chelator of intracellular Zn^{2+}. The elevation of $[GSH]_i$ could be caused by the increase in $[Zn^{2+}]_i$ in this preparation (Kinazaki et al., 2011). In the case of 10 μM HHQ, it is hypothesized that HHQ induces weak oxidative stress that converts thiols to disulfides, resulting in the release of small amount of Zn^{2+}, thus increasing cellular thiol content. The decrease in $[GSH]_i$ and increase in $[Zn^{2+}]_i$ by 3050 μM HHQ were presumed to increase cell vulnerability to oxidative stress induced by H_2O_2. However, HHQ at concentrations of 0.3–100 μM attenuated the H_2O_2-induced increase in cell lethality (Fig. 4). The addition of 3–10 μM $ZnCl_2$ did not augment the cytotoxicity of 10–30 μM HHQ.

Furthermore, HHQ seemed to delay the process of cell death induced by H_2O_2 (Fig. 5). Therefore, it is unlikely that Zn^{2+} is involved in HHQ-induced cytotoxicity, although HHQ increases $[Zn^{2+}]_i$. In a previous study (Kamae et al., 2017), HHQ at concentrations of 10 μM or more increased $[Ca^{2+}]_i$. HHQ at 10–30 μM significantly promoted the A23187-induced increase in cell lethality (Fig. 6). Therefore, Ca^{2+}, rather than Zn^{2+}, appears to be involved in the cytotoxicity of HHQ. HHQ exhibits opposing actions on cell death caused by oxidative stress and Ca^{2+} overload.

Toxicological implications of HHQ-induced increase in $[Zn^{2+}]_i$

HHQ is supposed to increase $[Zn^{2+}]_i$ in lymphocytes. Zn^{2+} is an intracellular messenger in lymphocytes (Haase and Rink, 2014). Although it is well known that zinc deficiency impairs immune functions (Shankar and Prasad, 1998; Haase and Rink, 2014), the influence of sustained increases in $[Zn^{2+}]_i$ on the immune system has not been elucidated. In the nervous system, however, dyshomeostasis of cellular Zn^{2+} (excessive increase or decrease in $[Zn^{2+}]_i$) is implicated in the pathogenesis of neurodegenerative disorders such as Alzheimer disease, Parkinson's disease, and schizophrenia (Szewczyk, 2013; Li and Wang, 2016). Thus, zinc homeostasis is critical in maintaining physiological neuronal functions. Since coffee (0.1–1.7 mg of HHQ per a cup) is consumed worldwide, large amounts of HHQ are ingested daily. HHQ at 1.26 mg/L (10 μM) can elevate $[Zn^{2+}]_i$ of rat thymocytes as shown in Fig. 1.

Quinones exert various simple and complex actions on cells, inducing cytoprotective and cytotoxic actions (Bolton and Dunlap, 2017). Therefore, it is not surprising that micromolar concentrations of HHQ seem to exert both beneficial and adverse actions on rat thymocytes. HHQ at 3–30 μM almost completely inhibited the H_2O_2-induced increase in cell lethality (Fig. 4), although at 30 μM, it significantly decreased $[GSH]_i$ (Fig. 3). One may argue the possibility that HHQ decomposes H_2O_2, resulting in reduced oxidative stress. However, this is unlikely

because of the following reasons. H_2O_2 also exerts high nucleophilicity, and can attack olefins to produce oxidation products. Although this reaction requires conjugated electron-withdrawing groups, HHQ has no electron-withdrawing group in its structure. Therefore, the possibility of direct reaction between H_2O_2 and HHQ is very low.

Conclusion

Micromolar concentrations of HHQ, known as a by-product of coffee bean roasting, exert diverse actions on rat thymic lymphocytes under present *in vitro* conditions. Although HHQ can significantly elevate $[Zn^{2+}]_i$ some actions are Zn^{2+}-independent. In addition, HHQ possesses contrasting effects on cell death caused by oxidative stress and Ca^{2+} overload. The pharmacokinetics of HHQ after the ingestion of coffee is not elucidated at present. However, HHQ-reduced coffee may be preferable to avoid possible adverse effects of HHQ.

Conflict of interest

All authors affirm that there are no conflicts of interest to declare.

Acknowledgements

This study was supported by Grants-in-Aid for Scientific Research (C26340039 and B15H02892) from the Japan Society for the Promotion of Science.

References

Bolton, J. L., Dunlap, T. (2016). Formation and biological targets of quinones: cytotoxic versus cytoprotective effects. Chem. Res. Toxicol. 30: 13−37.

Chikahisa. L., Oyama, Y., Okazaki, E., et al. (1996). Fluorescent estimation of H_2O_2-induced changes in cell viability and cellular nonprotein thiol level of dissociated rat thymocytes. Jpn J. Pharmacol. 71: 299–305.

Corsini, E., Sokooti, M., Galli, C. L., et al. (2013). Pesticide induced immunotoxicity in humans: a comprehensive review of the existing evidence. Toxicology 307: 123–135.

Fukunaga, E., Oyama, T. M., Oyama, Y. (2015). Elevation of the intracellular Zn^{2+} level by 2-n-octyl-4-isothiazolin-3-one in rat thymocytes: an involvement of a temperature-sensitive Zn^{2+} pathway. Toxicol. Res. 4: 65–70.

Gee, K. R., Zhou, Z. L., Qian, W. J., et al. (2002). Detection and imaging of zinc secretion from pancreatic beta-cells using a new fluorescent zinc indicator. J. Amer. Chem. Soc. 124: 776–778.

Haase, H., Rink, L. (2014). Zinc signals and immune function. Biofactors 40: 27–40.

Hojyo, S., Fukada, T. (2016). Roles of zinc signaling in the immune system. J. Immunol. Res. 2016: 6762343.

Kamae, R., Nojima, S., Akiyoshi, K., et al. (2017). Hydroxyhydroquinone, a by-product of coffee bean roasting, increases intracellular Ca^{2+} concentration in rat thymic lymphocytes. Food Chem. Toxicol. 102: 39–45.

Kinazaki, A., Chen, H., Koizumi, K., et al. (2011). Putative role of intracellular Zn^{2+} release during oxidative stress: a trigger to restore cellular thiol content that is decreased by oxidative stress. J. Physiol. Sci. 61: 403–409.

Klein, L., Kyewski, B., Allen, P. M., et al. (2014). Positive and negative selection of the T cell repertoire: what thymocytes see (and don't see). Nature Rev. Immunol. 14: 377–391.

Kuchler, L., Sha, L. K., Giegerich, A. K., et al. (2014). Sphingosine-1 phosphate promotes thymic atrophy during sepsis progression. Crit. Care, 18: P51.

Li, L. B. Wang, Z. Y. (2016). Disruption of brain zinc homeostasis promotes the pathophysiological progress of Alzheimer's disease. Histol. Histopathol. 31: 623–627.

Maret, W. (2009). Molecular aspects of human cellular zinc homeostasis: redox control of zinc potentials and zinc signals. Biometals 22:149–157.

Matsui, H., Oyama, T.M., Okano, Y., et al. (2010). Low micromolar zinc exerts cytotoxic action under H_2O_2-induced oxidative stress: Excessive increase in intracellular Zn^{2+} concentration. Toxicology 276: 27–32.

Matsui, H., Sakanashi, Y., Oyama, T. M., et al. (2008). Imidazole antifungals, but not triazole antifungals, increase membrane Zn^{2+} permeability in rat thymocytes: Possible contribution to their cytotoxicity. Toxicology 248: 142–150.

Müller, C., Hemmersbach, S., van't Slo, G., et al. (2006). Synthesis and structure determination of covalent conjugates formed from the sulfury-roasty-smelling 2-furfurylthiol and di- or trihydroxybenzenes and their identification in coffee brew. J. Agric. Food Chem. 54: 10076–10085.

Ochiai, R., Nagao, T., Katsuragi, Y., et al. (2008). Effects of hydroxyhydroquinone-reduced coffee in patients with essential hypertension. J. Health Sci.54: 302–309.

Park, J. S., Koentjoro, B., Veivers, D., et al. (2014). Parkinson's disease-associated human ATP13A2 (PARK9) deficiency causes zinc dyshomeostasis and mitochondrial dysfunction. Hum. Molec. Genet. 23: 2802–2815.

Poon, I. K., Lucas, C. D., Rossi, A. G., et al. (2014). Apoptotic cell clearance: basic biology and therapeutic potential. Nature Rev. Immunol. 14: 166–180.

Saitoh, S., Fukunaga, E., Ohtani, H., et al. (2015). Zn^{2+}-dependence of the synergistic increase in rat thymocyte cell lethality caused by simultaneous application of 4, 5-dichloro-2-octyl-4-isothiazolin-3-one (DCOIT) and H_2O_2. Chemosphere 135: 447–452.

Sakanashi, Y., Oyama, T.M., Matsuo, Y., et al. (2009). Zn^{2+}, derived from cell preparation, partly attenuates Ca^{2+}-dependent cell death induced by A23187, calcium ionophore, in rat thymocytes. Toxicol. In Vitro, 23: 338–345.

Shankar, A.H., Prasad, A.S. (1998). Zinc and immune function: the biological basis of altered resistance to infection. Ameri. J. Clin. Nutri. 68: 447S–463S.

Shimizu, S., Yoshida, T., Tsujioka, M., et al. (2014). Autophagic cell death and cancer. Intl. J. Molec. Sci. 15: 3145–3153.

Solti, I., Kvell, K., Talaber, G., et al. (2015). Thymic atrophy and apoptosis of CD4+ CD8+ thymocytes in the cuprizone model of multiple sclerosis. Plos One, 10: e0129217.

Szewczyk, B. (2013). Zinc homeostasis and neurodegenerative disorders. Frontiers in Aging Neurosci. 5: 33.

Yoo, M.H., Kim, T.Y., Yoon, Y.H., et al. (2016). Autism phenotypes in ZnT3 null mice: involvement of zinc dyshomeostasis, MMP-9 activation and BDNF upregulation. Sci. Rep. 6: 28548.

Figure legends

Figure 1. HHQ-induced augmentation of FluoZin-3 fluorescence in rat thymocytes. (A) Shift of FluoZin-3 fluorescence histogram 1 h after HHQ application. Each histogram was constructed with 2500 cells. (B) Dose-response relationship between HHQ and mean intensity of FluoZin-3 fluorescence. Column and bar were mean and SD, respectively, of four samples. Asterisks (**) show significant augmentation ($P < 0.01$) of FluoZin-3 fluorescence after HHQ application.

Figure 2. Modification of HHQ-elicited changes in FluoZin-3 fluorescence by Zn^{2+} chelators, DTPA for external Zn^{2+}, and TPEN for intracellular Zn^{2+}. Column and bar show mean and SD of four samples, respectively. Asterisks (**) show significant difference ($P < 0.01$) between the responses in absence and presence of respective Zn^{2+} chelator.

Figure 3. HHQ-induced changes in mean intensity of 5-CMF fluorescence in absence and presence of TPEN. Column and bar indicate mean and SD of four samples, respectively. Asterisks (**) show significant augmentation or attenuation ($P < 0.01$) of 5-CMF fluorescence after HHQ application. Symbols (##) show significant differences between responses in the absence and presence of TPEN.

Figure 4. Dose-responsive HHQ-induced protection of cells against oxidative stress elicited by H_2O_2. Column and bar indicate mean lethality and SD of four samples, respectively. Asterisks (**) show significant increase ($P < 0.01$) in cell lethality. Symbols (##) indicate significant attenuation of H_2O_2-induced increase in cell lethality.

Figure 5. Changes in cell population, classified with PI and annexin V-FITC, by treatment with H_2O_2, HHQ, and both. (A) Cytograms obtained from the cells treated with H_2O_2, HHQ, and both

for 2.5 h. Each cytogram was constructed with 2500 cells. Areas of *N*, *A*, *P*, and *AP* show the population of intact living cells, annexin V-positive living cells, dead cells, and annexin V-positive dead cells, respectively. (B) Percentage population (*N*, *A*, and *P* + *AP*) of cells treated with H_2O_2, HHQ, and both for 2.5 h. Column and bar indicate mean and SD of four samples, respectively. Asterisks (**) show significant increase or decrease ($P < 0.01$) by incubation with H_2O_2, HHQ, and both. Symbols (##) show significant differences between the cells treated with H_2O_2 alone and those co-treated with H_2O_2 and HHQ.

Figure 6. Effect of HHQ on cells simultaneously treated with 100 nM A23187. The cell lethality was estimated at 3 h after the start of application of A23187, HHQ, and both. Column and bar indicate mean and SD of four samples, respectively. Asterisks (**) show significant increase in cell lethality ($P < 0.01$) by incubation with H_2O_2, HHQ, and both. Symbols (##) show significant differences between the groups of cells treated with A23187 alone and cells co-treated with A23187 and HHQ.

Figure 1

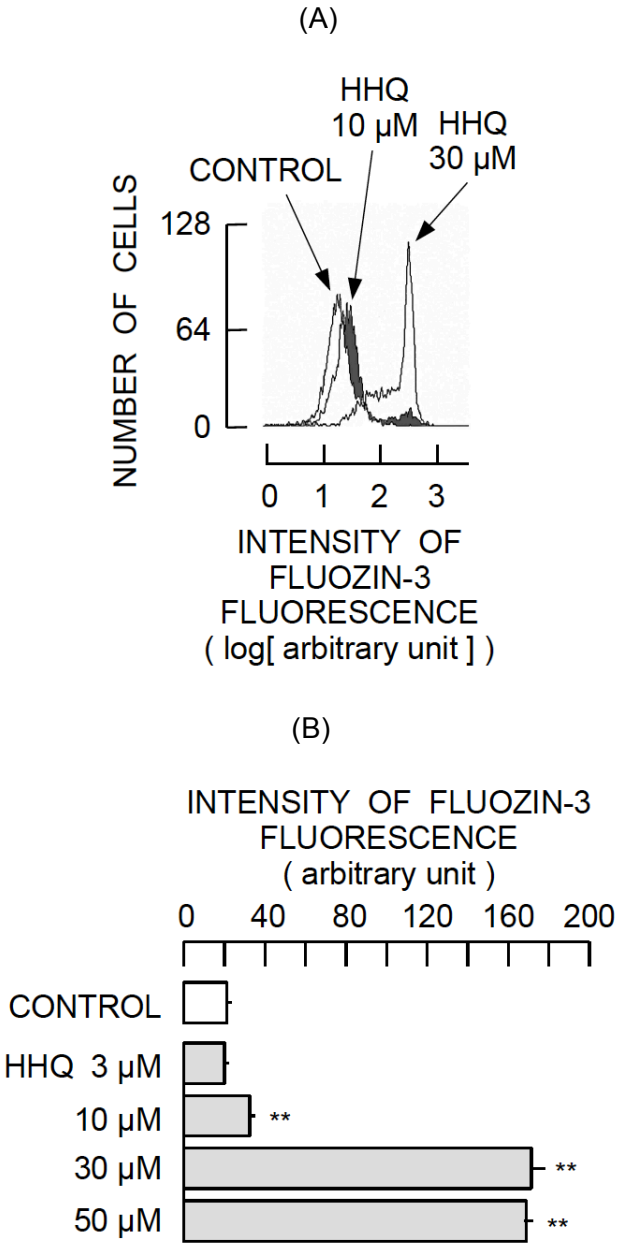
(A)
HHQ
10 μM
HHQ
30 μM
CONTROL
NUMBER OF CELLS
128
64
0
0 1 2 3
INTENSITY OF
FLUOZIN-3
FLUORESCENCE
(log[arbitrary unit])
(B)
INTENSITY OF FLUOZIN-3
FLUORESCENCE
(arbitrary unit)
0 40 80 120 160 200
CONTROL
HHQ 3 μM
10 μM
30 μM
50 μM
**
**
**

Figure 2

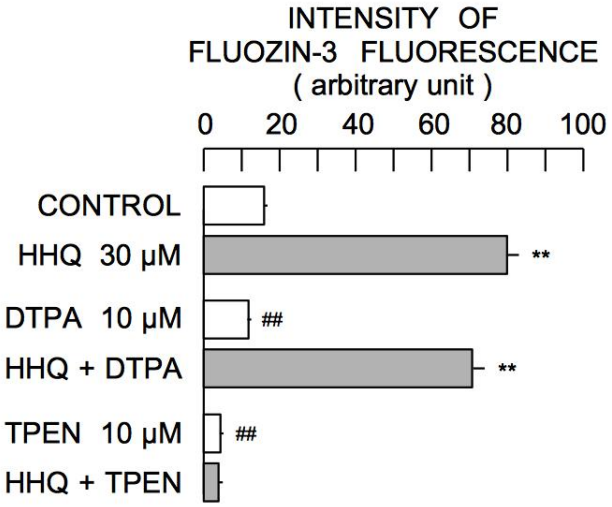
INTENSITY OF
FLUOZIN-3 FLUORESCENCE
(arbitrary unit)
0
20
40
60
80
100
CONTROL
HHQ 30 μM
**
DTPA 10 μM
##
HHQ + DTPA
**
TPEN 10 μM
##
HHQ + TPEN

Figure 3

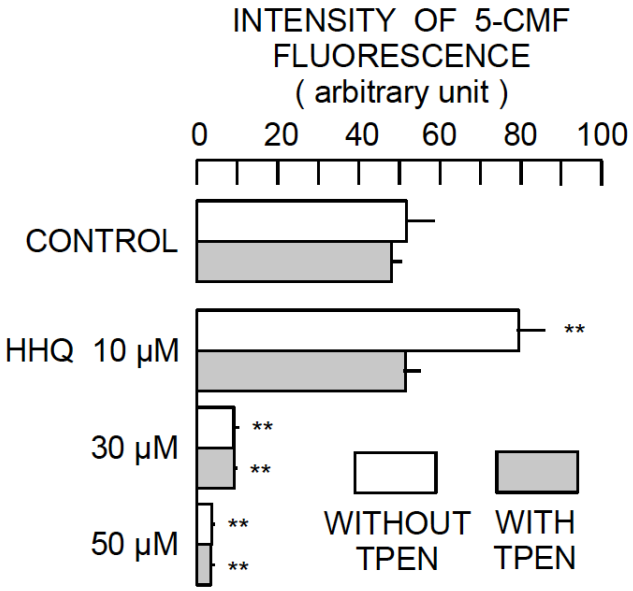
INTENSITY OF 5-CMF FLUORESCENCE
(arbitrary unit)
0
20
40
60
80
100
CONTROL
HHQ 10 μM
30 μM
50 μM
**
**
**
**
**
WITHOUT TPEN
WITH TPEN

Figure 4

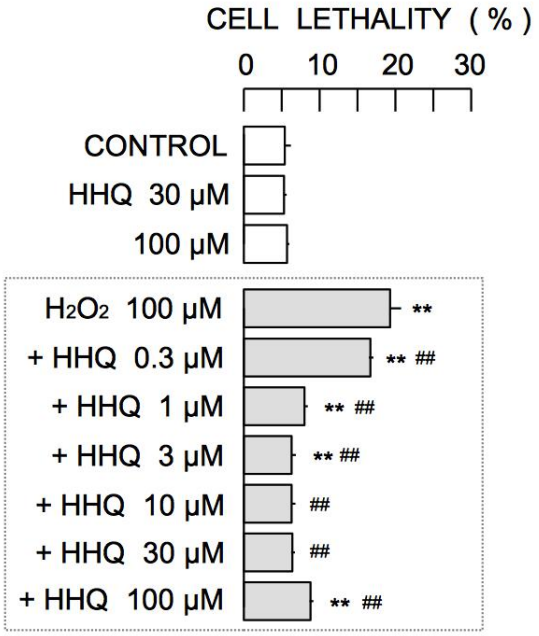
CELL LETHALITY (%)
0
10
20
30
CONTROL
HHQ 30 μM
100 μM
H2O2 100 μM
+ HHQ 0.3 μM
+ HHQ 1 μM
+ HHQ 3 μM
+ HHQ 10 μM
+ HHQ 30 μM
+ HHQ 100 μM
** ##
** ##
** ##
##
##
** ##

Figure 5

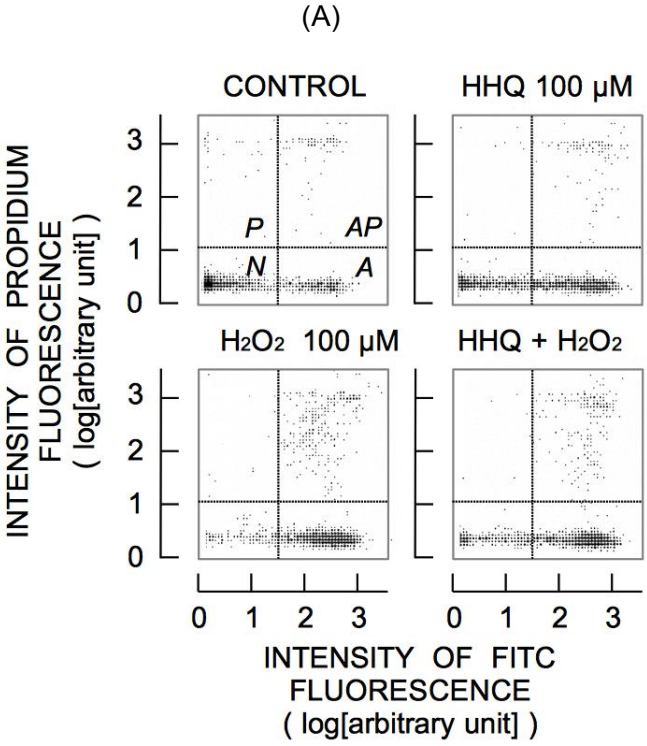
(A)
CONTROL
HHQ 100 μM
H2O2 100 μM
HHQ + H2O2
P
AP
N
A
INTENSITY OF PROPIDIUM FLUORESCENCE (log[arbitrary unit])
INTENSITY OF FITC FLUORESCENCE (log[arbitrary unit])
0
1
2
3

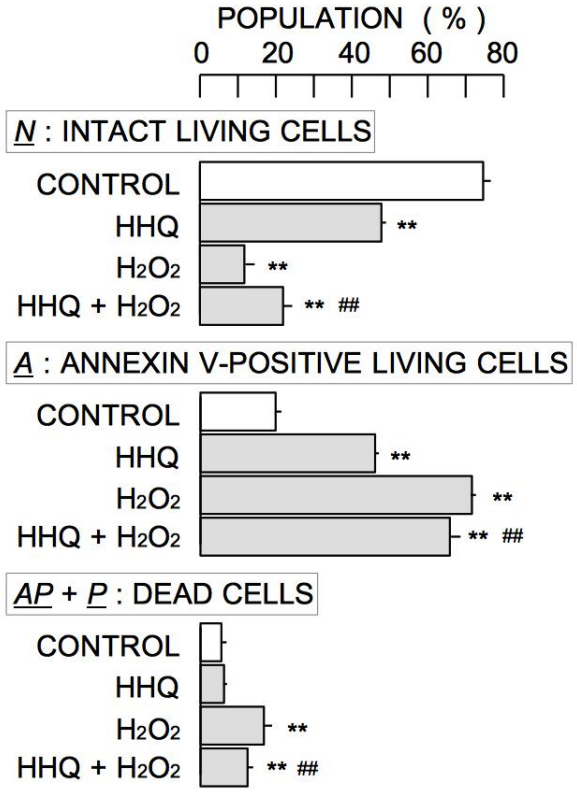
(B)
POPULATION (%)
0
20
40
60
80
N : INTACT LIVING CELLS
A : ANNEXIN V-POSITIVE LIVING CELLS
AP + P : DEAD CELLS
CONTROL
HHQ
H2O2
HHQ + H2O2
**
##

Figure 6

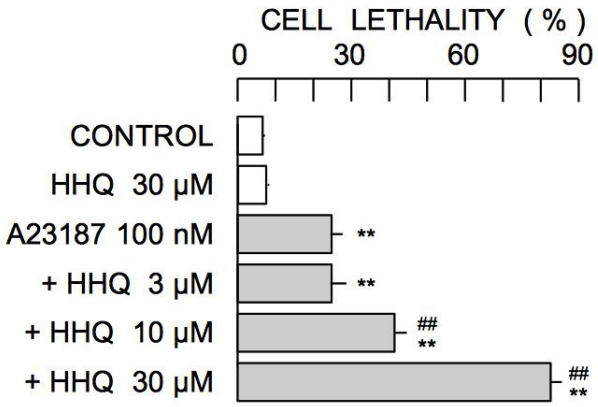
CELL LETHALITY (%)
0
30
60
90
CONTROL
HHQ 30 μM
A23187 100 nM
+ HHQ 3 μM
+ HHQ 10 μM
+ HHQ 30 μM
**
**
##
**
##
**

Table 1. Reagents used in this study

Chemical [Manufacturer]	Purpose
(1) Zinc Chelators	
Diethylenetriamine-N,N,N′,N″,N″-pentaacetic acid (DTPA)	Chelating extracellular Zn^{2+}
N,N,N′,N′-tetrakis(2-pyridylmethyl)ethylenediamine (TPEN)	Chelating intracellular Zn^{2+}
[Dojindo Chemical Laboratory, Kumamoto, Japan]	
(2) Fluorescent Probes	
Propidium iodide (PI)	Staining dead cells
FluoZin-3-AM	Estimating change in intracellular Zn^{2+} level
5-Chloromethylfluorescein diacetate (5-CMF-DA)	Estimating change in cellular glutathione content
[Molecular Probes, Inc., Eugene, OR, USA]	